DMD Fast Forward. Published on March 15, 2005 as doi:10.1124/dmd.104.001883

DMD #2004/001883RR

Species- and Disposition Model-Dependent Metabolism of Raloxifene in Gut and Liver: Role of UGT1A10*

Eun Ju Jeong[2], Yong Liu[3], Huimin Lin and Ming Hu[4]

Department of Pharmaceutical Sciences, College of Pharmacy, Washington State University, Pullman, Washington 99164 (EJJ, YL, HL, MH)

DMD Fast Forward. Published on March 15, 2005 as DOI: 10.1124/dmd.104.001883
This article has not been copyedited and formatted. The final version may differ from this version.

DMD #2004/001883RR

Running Title: Role of UGT1A10 in Raloxifene Metabolism

Authors:

Eun Ju Jeong, Yong Liu, Huimin Lin and Ming Hu

Address correspondence to:

Ming Hu, Ph.D.
Department of Pharmacological and Pharmaceutical Sciences
College of Pharmacy
University of Houston
Houston, TX 77030
Tel: (713)-795-8320
Fax :(713)-795-8305
Email: **mhu@uh.edu**

Number of Text Pages:	27
Number of Tables:	3
Number of Figures:	7
Number of References:	35
Number of Words in Abstract:	248
Number of Words in Introduction:	610
Number of Words in Discussion:	1199

ABBREVIATIONS: HBSS, Hank's balanced salt solution; SERM, selective estrogen receptor modulator; UGT, UDP-glucuronosyltransferase

DMD Fast Forward. Published on March 15, 2005 as DOI: 10.1124/dmd.104.001883
This article has not been copyedited and formatted. The final version may differ from this version.

ABSTRACT

Caco-2 cell lysate, and intestinal and liver microsomes derived from female humans and rats were used to compare and contrast the metabolism and disposition of raloxifene. In Caco-2 cell lysate, raloxifene 6-β-glucuronide (M1) was the main metabolite, although raloxifene 4'-β-glucuronide (M2) was formed in comparable abundance (58% versus 42%). In rat liver and intestinal microsomes, M1 represented about 76-86% of glucuronidated metabolites. In contrast, raloxifene 4'-β-glucuronide (M2) was the predominant metabolite in expressed UGT1A10 (96%) and human intestinal (92%) microsomes. Intrinsic clearance for M2 ($CL_{int, M2}$) in human intestinal microsomes was 33-72 folds higher than in rat microsomes, whereas intrinsic clearance for M1 ($CL_{int, M1}$) was 3-4 folds lower. Taken together, total intrinsic clearance ($CL_{int, M1} + CL_{int, M2}$) in human intestinal microsomes was 3-6 folds higher than rat intestinal microsomes, but was similar in liver microsomes. In addition, intrinsic clearance in small intestinal microsomes was 2~5 folds higher than that in hepatic microsomes, regardless of species. To account for the difference in species- and disposition model-dependent intestinal metabolism, we probed the presence of various UGT1A isoforms in Caco-2 cells using real-time RT-PCR, and as expected detected no UGT1A10. In conclusion, the lack of UGT1A10 may explain why Caco-2 cell and rat intestinal microsomes metabolized raloxifene differently from human intestinal microsomes. The presence of human intestinal UGT1A10 and higher overall intrinsic clearance value in the human intestine as the result of UGT1A10 expression could explain why raloxifene has much lower bioavailability in humans (2%) than in rats (39%).

DMD Fast Forward. Published on March 15, 2005 as DOI: 10.1124/dmd.104.001883
This article has not been copyedited and formatted. The final version may differ from this version.

Raloxifene, a member of selective estrogen receptor modulators (SERMs), is a drug for the treatment and prevention of osteoporosis in postmenopausal women (Heringa, 2003). It is also undergoing clinical trial for breast cancer prevention. Sixty-two to seventy percent of postmenopausal women are potential candidates for SERMs, and the percentage of actual users is expected to rise as a hormone replacement therapy trial recently yielded disappointing negative results (Rossouw et al., 2002; Lacey Jr et al., 2002).

The bioavailability of raloxifene was reported to be very low (2%) in humans, even though it has oral efficacy in osteoporosis. This may represent a significant challenge to its possible future use as a chemopreventive agent. It is generally believed that absorption is not the main reason for poor bioavailability since approximately 60% of dose was absorbed after oral administration (Hochner-Celnikier, 1999), (Eli Lilly, 1998; Snyder et al., 2000). However, we found recently that raloxifene was effluxed by various transporters such as multidrug resistance related protein (MRP) and organic anion transporter (OAT), which could contribute to its poor bioavailability (Jeong et al, 2004). More importantly, we also found that raloxifene is extensively conjugated (about 90% at concentrations less than 10 μM) during transport across the Caco-2 cell monolayer (Jeong et al, 2004), consistent with previous observation that raloxifene undergoes extensive phase II metabolism in the gut (Kemp et al, 2002). However, the main metabolites in Caco-2 cells were sulfates whereas the primary metabolite in humans is raloxifene 4'-β-glucuronide or M2. In humans, plasma concentration of 4'-β-glucuronide is 8-fold higher than 6-β-glucuronide or M1 (Jones, 1997).

In contrast to its poor bioavailability in humans, raloxifene has fairly good bioavailability in rats (39%) (Lindstrom et al., 1984). This is somewhat unexpected since the major metabolic pathway in rats is also glucuronidation. Upon further examination, the major metabolite in rats was found to be M1 (Lindstrom et al., 1984), similar to what we found for Caco-2 cell glucuronidation of raloxifene (Jeong et al, 2004). Because many of the pharmacodynamic studies of raloxifene are conducted in rats (Zheng et al., 2004; Ozgonul et al., 2003; Cao et al., 2002; Kubatka et al., 2001; Merchenthaler et al., 1998), it would be important to resolve why there were these important species difference in raloxifene disposition. Therefore, the main purpose of the present study is to determine how species and disposition model choice affect the intestinal and hepatic disposition of raloxifene. Our results indicate for the first time that lack of UGT1A10 expression is the main reason why 4'-β-glucuronide is not the main metabolite in rats and Caco-2 cells, and may explain the species-dependent disposition of raloxifene.

As a part of characterization work on raloxifene metabolism, we also measured the drug interactions potentials between raloxifene and flavonoids. Flavonoids especially isoflavones are taken as dietary supplements by women who experienced symptoms associated with menopause, which can be worsen by raloxifene administration. Therefore, a combination of flavonoids and raloxifene is expected to be taken by postmenopausal women (Crisafulli et al., 2004a,b, Kreijkamp-Kaspers et al., 2004, Cotter and Cashman 2003, Goodman-Gruen and Kritz-Silverstein 2003). A concern arising from this possible combination is that metabolism of raloxifene is similarly to that of flavonoids. Both are extensively metabolized in gut via phase II conjugations (Crespy et al., 1999; Walle et al, 1999; Andlauer et al., 2000; Liu and Hu, 2002; Chen et al, 2003; Jia et al, 2004).). Therefore, we determined the potential for interactions

between selected flavonoids (e.g., genistein and apigenin) and raloxifene using the microsomes. Our results indicated there is a moderate chance of beneficial interactions in the gut wall but not in liver, which could lead to a higher raloxifene bioavailability in vivo.

MATERIALS AND METHODS

Materials. Raloxifene was extracted from Evista® tablet (Eli Lilly and Company, Indianapolis, IN) using 100% ethanol and concentration was then verified by using authentic raloxifene hydrochloride purchased from National Cancer Institute Chemical Standard Repository managed by Midwest Research Institute (Kansas City, MO). Uridine diphosphoglucuronic acid, alamethicin, disaccharic-1, 4-lactone monohydrate, magnesium chloride, Tris and Hanks' balanced salt solution (HBSS) were products of Sigma-Aldrich (St. Louis, MO). Female human liver microsome and human UGT1A10 supersomes were purchased from BD Biosciences (Woburn, MA) and female human jejunal and ileal microsomes were obtained from Tissue Transform Technologies (Edison, NJ). Cloned Caco-2 cells (TC7) were a kind gift from Dr. Moniqué Rousset (Institute National de la Santé et de la Recherche zU178, Villejuit, France). All other materials were analytical grade or better and used as received.

Cell Culture. Cell culture conditions for growing Caco-2 cells have been described previously (Liu and Hu, 2002; Hu et al., 1994a,b; Chen et al., 2003; Jeong et al., 2004). The seeding density was 100,000 cells/cm^2 (4.2 cm^2 per monolayer) and Dulbecco's modified Eagle's medium supplemented with 10% fetal bovine serum was used as the growth media. Quality control criteria were the same as described previously (Hu et al., 1994a,b). Cell monolayers from 19 to 22 days past seeding were used for the experiments.

Preparation of Caco-2 Cell Lysate. After six mature (19-22 days post-seeding) Caco-2 cell monolayers were washed twice with 3 ml of 37ºC HBSS (pH 7.4), they were cut out together

with the porous polycarbonate membranes, immersed into 6 ml of 50 mM potassium phosphate buffer (pH 7.4) and sonicated in an ice bath (4ºC) for 30 min as described previously (Jeong et al., 2004). Afterwards, the cell lysate was centrifuged at 1000 rpm for 5 min to remove the polycarbonate membrane. The protein concentrations of the cell lysate were then determined using a commercial protein assay kit (Bio-Rad, Hercules, CA).

Real-Time Quantitative RT-PCR Analysis of UGT1As. Standard reagents and methods were used to perform quantification of UGT1A mRNA levels using reverse-transcriptase and SYBR® Green Dye. The followings are a brief description of the procedures.

RNA Isolation. Small amounts of total RNA were extracted from Caco-2 cells using a commercial RNA isolation kit (Ambion, Austin, TX), whereas large amounts of total RNA from $5x10^8$ cells were extracted using TRIzol® reagent (Invitrogen, Carlsbad, CA). RNA concentration and purity was determined by OD_{260} and OD_{280} readings, and RNA integrity was monitored by agarose gel electrophoresis. Prior to RT-PCR and real-time PCR, contaminating DNA in RNA samples and excess DNase were removed using DNA-free™ DNase Treatment & Removal Reagents (Ambion, Austin, TX). To monitor for possible DNA contamination, PCR amplification of β-actin cDNA was performed using a primer pair (5'-ggcggcaccaccatgtaccct-3'and 5'-cgatccacacggagtacttgc-3') that span intron 5 of that gene. Genomic DNA template leads to a 312–bp product and the cDNA template generates a 202-bp product. In the absence of genomic DNA in the RNA samples, the 202-bp PCR product is only expected in the RT-PCR sample. Extracted RNA samples free from DNA were stored at –80ºC until real-time PCR analysis.

Reverse Transcription. Synthesis of first-strand cDNA was carried out using SUPERSCRIPT™ III, RNase H- Reverse Transcriptase (RT) (Invitrogen, Carlsbad, CA).

Oligonucleotide Primers for real-time RT-PCR. Primers for the amplification of the human UGT RNA transcripts as well as for β–actin sequences were generated using standard molecular biology software (Table 1). The UGT primers are either specific for regions in each of unique exon 1 sequences, or for sequences that are common to several (e.g., UGT1A7-UGT1A10) or all of the UGT1A RNAs (Table 1).

Real-Time PCR. Real-time quantitative PCR was performed using the GeneAmp® 5700 Sequence Detection System (Applied Biosystems, Foster City, Calif.) and carried out using SYBR® Green as the quantification tool according to the manufacturer's instruction. The final concentration of each forward or reverse oligonucleotide primer in the PCR mixture was 200 nM. PCR assays for constructing standard curves were performed in triplicate, while the remaining PCR assays were performed in duplicates, both in three separate replicate runs. The concentrations of the primers and templates were optimized, and the final PCR conditions were as follows: 95ºC for 10 min, followed by 40 cycles consisting of 95ºC for 15 s, and 60ºC for 1 min. Data acquisition and analysis were handled by the built-in software (Applied Biosystems).

Data Analysis in RT-PCR and Real-Time PCR Methods.

Semiquantitative RT-PCR for UGT Detection. To detect the different isoforms of UGT, PCR was conducted using UGT specific sense and antisense primers (ß-actin primers were added as an internal reference). PCR for experiments with cultured cells were performed with 0.5 U of Highfidelity *Taq* DNA polymerase (Invitrogen) on 4 to 10 µl of cDNA under the following

conditions: 94°C for 5 min, and then followed by 30 cycles consisting of a 30-s denaturing step at 94°C, a 45-s annealing step at 58°C, and a 45-s elongation step at 72°C in a thermal cycler (MJ Research, Reno, NV). The products were separated in a 1.5% agarose gel that contained ethidium bromide. The bands were visualized under UV light and photographed with a computer-assisted camera. The specificity of all primer pairs was confirmed through sequencing or restriction analysis of the PCR products.

Real–Time RT-PCR. Briefly, a threshold was assigned to the log phase of product accumulation. The point at which the threshold crosses the amplification curve is defined as a cycle threshold value, termed CT. With increasing target quantity in the PCRs, the CT value decreases linearly, and thus CT values can be used as relatively quantitative measurements of the input target amount. For the present determination, the threshold value was set at 0.4 (for UGT in Caco-2 cells), which was significantly above the background noise, and the numbers of cycles required to reach this CT value were determined.

Animals. Female Sprague-Dawley rats (70 ~ 110 days old, body weight 240 ~ 260 g, Simonsen Laboratory, Gilroy, CA) were fed with Teklad F6 rodent diet (Harlan Laboratories, Madison, WI). The rats were fasted overnight before the day of experiment.

Preparation of Rat Intestinal and Liver Microsomes. The protocols for preparing rat intestinal and liver microsomes were similar to those described previously (Chen et al., 2003).

UGT Metabolism Studies. Glucuronidation of raloxifene by Caco-2 cell lysate as well as intestinal and liver microsomes was measured using procedures described previously (Chen et al, 2003; Jeong et al., 2004). The microsome fraction or Caco-2 cell lysate (final concentration ~ 0.05 mg protein/ml in reaction mixture) was mixed with magnesium chloride (0.88 mM), saccharolactone (4.4 mM) and alamethicin (0.022 mg/ml). Raloxifene (final concentration 0 ~ 34.7 μM) or raloxifene (4.34 μM) plus apigenin or genistein (final concentration 0 ~ 100 μM) in 50 mM potassium phosphate buffer (pH 7.4) was then added. Uridine diphosphoglucuronic acid (3.5 mM) was added last to the reaction mixture (total volume 200 μl) to initiate reaction. The mixture was incubated in a 37ºC shaking (200 rpm) water bath for 30 ~ 60 min for intestinal and liver microsomes and 4 h for Caco-2 cell lysate. The final organic solvent concentration was 1% (1% ethanol for raloxifene or 0.95% ethanol plus 0.01% DMSO for raloxifene with flavonoids). The reaction was stopped by the addition of 40 μl solution of 6% glacial acetic acid in acetonitrile containing 100 μM of testosterone as the internal standard.

HPLC Analysis of Raloxifene and its Conjugates. The HPLC conditions were same as described before (Jeong et al., 2004). The retention times for raloxifene, 6-β-glucuronide, 4'-β-glucuronide, and internal standard (testosterone) were 13.6, 7.2, 9.8 and 21.4 min, respectively (Fig. 1).

Data Analysis in Microsome Model. Metabolic rates (V) were plotted against raloxifene concentration (C) in the final reaction mixture. Apparent K_m, V_{max} and intrinsic clearance (CL_{int}) were obtained via nonlinear regression analysis of the Michaelis-Menten equation (or equation 1).

$$V = \frac{V_{max} \times C}{C + K_m} \qquad (1)$$

$$CL_{int} = \frac{V_{max}}{K_m} \qquad (2)$$

For rat intestinal microsomes which showed substrate inhibition on Eadie-Hofstee plots, the kinetic parameters were calculated according to equation (3) using ADAPT II program (D' Argenio and Schumitzky, 1997).

$$V/C = \frac{V_{max}}{(C + K_m + (C^2 / K_{si}))} \qquad (3)$$

In equation (3), K_{si} is the constant describing the substrate inhibition (Houston and Kenworthy, 2000), whereas other terms are the same as described previously. Equation (3) was used by Houston and Kenworthy (2000) to describe substrate inhibition in a two binding site model.

For the inhibition study with flavonoids, % control of the metabolic rates (V) was plotted against flavonoid concentration in the final reaction mixture. Apparent IC_{50} values, or the inhibitor concentration at which the metabolic rate was decreased 50% when compared to the control, were calculated by fitting the data to a classical IC_{50} equation using nonlinear regression (a SigmaPlot™ function).

Statistical Analysis. Student's *t*-test (Microsoft Excel) was used to analyze the data. The prior level of significance was set at 5%, or $p < 0.05$.

RESULTS

Metabolism of Raloxifene in Caco-2 Cell Lysate. Caco-2 cell lysates were incubated with raloxifene (4.34 μM) for 4 hr in glucuronidation reaction , and the results indicated that there were two main glucuronide peaks (M1 and M2), as previously reported (Jeong et al., 2004a). Sulfates were not observed using Caco-2 cell lysate since coenzymes for sulfotransferases were not added to the incubation mixture. Between the two glucuronides (6- β-glucuronide and 4'-β-glucuronide (Jones, 1997)), M2 was identified as 4'-β-glucuronide, because M2 was the main metabolite formed by UGT1A10 (Fig. 1 and later). In comparing the rates of metabolism, we found that raloxifene 6-β-glucuronide (M1) was formed at a rate of 0.626±0.075 pmol/min/mg protein, 40% faster than the formation rate of raloxifene 4'-β-glucuronide (M2). The actual percentages of metabolites found at the end of the 4 hr experiment were 58% (M1) versus 42% (M2).

Relative Expression of UGT Isoforms in the Caco-2 Cells. To explain the difference seen in Caco-2 cell lysate and what is expected based on reported rapid metabolism in human intestinal microsomes (Kemp et al, 2002), we determined the relative expression levels of UGT isoforms in Caco-2 cell lysate using a real-time RT-PCR method. The results indicated that UGT1A1, UGT1A3, UGT1A4, UGT1A5, UGT1A6, and UGT1A8 and UGT1A9 isoforms were expressed in Caco-2 cells, whereas UGT1A7 and UGT1A10 were not (Fig.2). Among the UGT1A isoform mRNAs expressed by Caco-2 cells, UGT1A6 was the most abundant, followed by UGT1A3, UGT1A1, UGT1A5, UGT1A4, and UGT1A9. Based on CT values, the relative

expression levels of these isoforms are UGT1A6 (26):UGT1A3 (1.5):UGT1A1 (1.0):UGT1A5 (0.72): UGT1A4 (0.54): UGT1A9 (0.24):UGT1A8 (0.01).

Metabolism of Raloxifene in Human Microsomes. Raloxifene glucuronidation was determined using pooled female human intestinal (jejunal and ileal) and liver microsomes along with expressed human UGT1A10 microsome to further define the role of UGT1A10 in organ-specific metabolism of raloxifene.

Human jejunal and ileal microsomes were found to mainly metabolize raloxifene to M2, different from raloxifene glucuronidation in Caco-2 cell lysate. M2 is also the main metabolite in expressed human UGT1A10 (96%) (Fig.3). Previously, Kemp et al. (2002) showed that UGT1A10 displayed complete selectivity for M2 formation. In contrast, substantial amounts of M1 were found in liver microsomes (41% M1 versus 59% M2, Fig.3).

In intestinal microsomes, M2 formation displayed significantly larger V_{max} value (9.1~11 fold) and higher intrinsic clearance (14~16 fold) values than M1 formation (Table 2 and Fig. 4). In liver microsomes, M2 formation was associated with faster intrinsic clearance ($CL_{int, M2}$, 2.5 fold), but smaller V_{max} values (34% less) when compared to M1 formation (Table 2 and Fig. 4).

When comparing M1 formation by microsomes prepared from different organs/tissues, we found that liver microsomes displayed the highest apparent K_m and V_{max} value. As consequence, it has the largest apparent $CL_{int, M1}$ (1.2~1.7 fold) values (Table2 and Fig. 4A). For M2 (the main metabolite) formation, intestinal microsome displayed apparent K_m values similar to liver, but had significantly higher V_{max} values (5.0~5.2 fold) and apparent $CL_{int, M2}$ (3.9~4.9 fold) values when compared to liver (Table 2 and Fig. 4B).

Metabolism of Raloxifene in Rat Microsomes. Rates of glucuronidation were also determined using female rat intestinal microsomes prepared from four different regions (duodenum, jejunum, ileum and colon) and liver microsomes to determine the possible regional difference in the metabolism of raloxifene and to contrast the results with those obtained from humans.

In rat microsomes, the main metabolite was M1 (82% in liver; 76~86% in intestine) (Fig. 2). The apparent K_m values for M1 formation was lower than M2 formation in intestinal microsomes other than colonic microsomes, and the difference ranged from approximately 4 to 10 folds. K_m values in colonic microsomes were similar. In all intestinal microsomes, the apparent V_{max} values for M1 formation were higher (14% to ~700%) than M2 formation. In liver microsomes, M1 formation displayed apparent K_m values that were 44% lower and the apparent V_{max} values that were 3.8 fold higher than M2 formation (Table 2).

In rat intestinal micrsosomes, raloxifene was glucuronidated in all four sites with highest apparent CL_{int} in duodenum and lowest apparent CL_{int} in ileum for both M1 and M2 (Table 2). Eadie-Hofstee plots showed substrate inhibition at high substrate concentrations in all sites (Fig. 6), and therefore equation (3) were used to obtain kinetic parameters (Table 2). For M1 formation, duodenal and jejunal microsomes displayed lower apparent K_m values (0.5~0.8 fold) but higher apparent $CL_{int, M1}$ value (1.5~1.6 fold) than liver (Table 2 and Fig. 5). For M2 formation, duodenal and jejunal microsome displayed higher apparent K_m values (2.7 fold) than liver but similar apparent $CL_{int, M2}$ values (Table 2 and Fig. 5). On the other hand, ileal and colonal microsomes have lower apparent K_m, $CL_{int, M1}$ and $CL_{int, M2}$ values (Table 2 and Fig. 5).

When we compared raloxifene metabolism in human and rat microsomes, we found that the apparent $CL_{int, M1}$ in human was only 24~41% of rat, but apparent $CL_{int, M2}$ was substantially higher in human (5.6 fold in liver, 33 fold in jejunum, 72 fold in ileum) than in rat (Table 2). Taken together, the total apparent CL_{int} (sum of $CL_{int, M1}$ and $CL_{int, M2}$) of raloxifene in human intestinal microsomes was higher than the corresponding rat intestinal microsomes (3.3 fold for jejunum and 6.2 fold for ileum). On the other hand, the total apparent CL_{int} in human liver microsomes was almost the same as the rat liver.

Effects of Flavonoids on Raloxifene Metabolism. The results indicated that metabolism of raloxifene in the rat microsomes, Caco-2 cell lysate and human microsomes can be significantly and substantially decreased by the presence of genistein and apigenin (Fig. 7). Furthermore, the apparent IC_{50} values were in the range of 1-10 μM for Caco-2 cell lysate and rat microsomes (Table 3). In human intestinal microsomes, the apparent IC_{50} values were much higher (15-50 μM) (Table 3).

DISCUSSION

Disposition of raloxifene is likely to have profound effects on its anticipated anticancer indication since consistent exposure levels are needed to sustain chemopreventive effects. Preclinical studies exploring raloxifene's anticancer effects have used rodents (e.g., rats) as its primary model (Zheng et al., 2004; Ozgonul et al., 2003; Cao et al., 2002; Kubatka et al., 2001; Merchenthaler et al., 1998). Because of the substantial difference in the metabolism of raloxifene (e.g., 39% bioavailability in rats and 2% in humans), the results derived from rodents must be weighed carefully before extrapolating to humans. This is because, in addition to typical species differences in pharmacological and pharmacodynamic responses, there are likely to be substantial difference in their pharmacokinetic responses as the result of disposition differences.

The first difference in disposition is the expression level of UGT1A10 in different species. UGT1A10 is the isoform responsible for M2 formation and rapid raloxifene clearance. Our result clearly demonstrated that UGT1A10 is a major isoform responsible for the selective formation of raloxifene 4'-β-glucuronide (M2) over M1, which is consistent with an earlier observation using human microsomes (Kemp et al, 2002). Its absence from the rats could largely, albeit not completely, explain why the extent of metabolism of raloxifene in rats is lower than humans. In other words, the substantial difference in (intrinsic) clearance of M2 in the intestine of rats versus humans (with rat's clearance being 33~72 fold less) clearly supercedes the fact that M1 clearance in rats is much faster (3~4 folds) than that in humans (Table 2).

The second difference is where UGT1A10 is expressed. The presence of UGT1A10 in the human intestine and their absence from the human liver (Strassburg et al., 1999; Tukey and Strassburg, 2000) explains the higher formation rates of M2 and higher intrinsic glucuronidation clearance in humans than in rats. It also explains why rat intestine did not have much higher intrinsic clearance than rat liver. Similarly, in Caco-2 cells, which express UGT1A1, UGT1A3, UGT1A4, UGT1A6, and UGT1A8 (very low level) but not UGT1A10 (Fig.2), much less M2 is formed than M1. The latter is somewhat unexpected since these cells were derived from human colon adenocarcinoma cells. Human colonic enterocytes were reported to express UGT1A1, UGT1A3, UGT1A4, UGT1A6, UGT1A8, UGT1A9 and UGT1A10 mRNA (Tukey and Strassburg, 2000, Strassburg et al., 1998 and 2000).

The third difference is where and how much UGT1A8 is expressed. Previously, UGT1A8 were reported to catalyze both M1 and M2 formation (Kemp et al., 2002). Since UGT1A8 is only expressed in human intestine, it helps to explain why there was more extensive metabolism of raloxifene in intestine than in liver. On the other hand, its ability to catalyze the formation of both M1 and M2 explain why M1 is present in the human intestinal microsome experiments. Formation of M1 may be aided by the presence of UGT1A1, which is known to be expressed by both liver and intestine. Taken together, UGT1A8 and to a lesser extent UGT1A1 in both human and rat (King et al., 2000) were responsible for M1 formation.

The fourth difference is probably the transporters which are responsible for the excretion of phase II conjugates and how they control the cellular excretion of phase II metabolites. This is becoming a more important issue, especially in our recent investigation of flavonoid and

raloxifene disposition, where efflux transporters often serve as a "gate keeper" or "the rate-limiting step" in cellular excretion of flavonoid and raloxifene conjugates (Chen et al, 2003; Hu et al, 2003; Jeong et al, 2004; Chen et al, 2004). In the present study, M1 was main metabolite in Caco-2 cell lysate (60%). This is very different from our previous observation in intact Caco-2 cell monolayers, where M2 was main glucuronide excreted by the Caco-2 cells (Jeong et al, 2004). It is probable that M1 is not well transported by the efflux transporter or its efflux is competitively inhibited by raloxifene itself (a MRP2 substrate, Jeong et al, 2004). An additional possibility is that raloxifene sulfate produced in Caco-2 cells at a much higher concentration (than glucuronide) inhibited the efflux of M1. Additional studies are necessary to delineate the mechanisms responsible for this unexpected difference.

Taken together, these differences in disposition strongly support the role played by intestine in the first-pass metabolism of raloxifene. The results of present study clearly showed the substantial preference (14~16 fold higher CL_{int}) for M2 over M1 in human intestine. This preference (or difference in $CL_{int, M2}$) is larger than 6 fold difference observed by Kemp et al (2002) in human intestinal jejunal microsomes. Specifically, our results contained substantially smaller (>10 times lower) K_m values although the V_{max} values were comparable (<3 times less). Multiple factors could contribute to this difference in the extent of preference, including the sources of human intestinal microsomes, concentrations of raloxifene used in the reaction (we could not reach 40 μM without using more than 1% organic phase), and methods of estimating K_m where Kemp et al (2002) used truncated rates versus concentrations data and Michaelis-Menten equation to get K_m. Despite the above differences, both sets of results are consistent with an earlier observation that M2 concentration in human systemic circulation was 8- fold

higher than M1 (Jones et al, 1997). On the other hand, data from this study indicate that a lack of UGT1A10 expression in the rat intestine is a likely mechanism for increased raloxifene bioavailability in rats.

Lastly, we investigated the potential metabolic interaction between raloxifene and flavonoids since they are are likely to be taken together by post-menopausal women. The results showed that the potentials for metabolic interaction between raloxifene and flavonoids (genistein and apigenin) in the intestine clearly exit. The apparent IC_{50} value of flavonoids in the ten's of μM range (Fig. 7 and Table 3) is achievable by the consumption of dietary supplement (Setchell et al., 2001; Setchell et al., 2003), especially in the intestinal lumen. Based on our previous experience, apigenin can easily achieve this apparent IC_{50} concentration in the lumen whereas genistein can also achieve its IC_{50} concentration, although some formulation manipulation may be needed (Liu and Hu, 2002). Therefore, these isoflavones have the potential to increase the bioavailability of raloxifene when taken together. The higher inhibitory effect of apigenin over genistein may be explained by the fact that apigenin is a better substrate for various UGT isoforms (e.g. UGT1A1, UGT1A8 and UGT1A9) (King et al., 2000). The higher apparent IC_{50} values (8 ~ 52 μM) exhibited by genistein against raloxifene glucuronidation suggests that the potential for metabolic interaction between raloxifene and genistein is low. Taken together, we did not expect to observe substantial interaction between raloxifene and flavonoids in humans since flavonoids did not appear to substantially inhibit raloxifene glucuronidation in UGT1A10-rich human intestinal microsomes at physiological concentrations.

In conclusion, the intestinal phase II metabolism catalyzed by UGT1A family plays a more significant role in the extensive first-pass metabolism of raloxifene than hepatic metabolism in both humans and rats. The contribution of intestinal metabolism to low bioavailability of raloxifene is more prominent in humans than in rats because of abundance of UGT1A10 isoform in the human intestine. Isoflavones and flavones have moderate potential to improve the bioavailability of raloxifene by inhibiting the intestinal conjugation of raloxifene.

REFERENCES

Andlauer W, Kolb J, and Furst P (2000) Isoflavones from tofu are absorbed and metabolized in the isolated rat small intestine. *J Nutr.* **130:**3021-3027.

Cao Y, Mori S, Mashiba T, Westmore MS, Ma L, Sato M, Akiyama T, Shi L, Komatsubara S, Miyamoto K, Norimatsu H (2002) Raloxifene, estrogen, and alendronate affect the processes of fracture repair differently in ovariectomized rats. *J Bone Miner Res*. **17:**2237-46.

Chen J, Lin H and Hu M (2003) Metabolism of flavonoids via enteric recycling: role of intestinal disposition. *J Pharmacol Exp Ther.* **304**:1228-1235.

Chen J, Lin H and Hu M (2004) Absorption and Metabolism of Genistein and Its Isoflavone Analogs in Human Intestinal Caco-2 Cells. Cancer Chemotherap. Pharm., *in press.*

Court MH, Duan SX, von Moltke LL, Greenblatt DJ, Patten CJ, Miners JO, Mackenzie PI (2001) Interindividual variability in acetaminophen glucuronidation by human liver microsomes: identification of relevant acetaminophen UDP-glucuronosyltransferase isoforms. *J Pharmacol Exp Ther.* **299**:998-1006.

Crespy V, Morand C, Manach C, Besson C, Demigne C, and Remesy C (1999) Part of quercetin absorbed in the small intestine is conjugated and further secreted in the intestinal lumen. *Am J Physiol.* **277:**G120-G126.

D' Argenio, D. Z. & Schumitzky, A. (1997). ADAPT II user's guide: pharmacokinetic / pharmacodynamic systems analysis software. Biomedical simulations resource, University of Southern California, Los Angeles.

Eli Lilly (1998), Raloxifene package insert.

Heringa M (2003) Review on raloxifene: profile of selective estrogen receptor modulator. *Int J Clin Pharmacol Ther*. **41**(8):331-345.

Hochner-Celnikier D (1999) Pharmacokinetics of raloxifene and its clinical application. *Eur J Obstet Gynecol Reprod Biol.* **85**:23-29.

Houston JB, Kenworthy KE. (2000) In vitro-in vivo scaling of CYP kinetic data not consistent with the classical Michaelis-Menten model. *Drug Metab Dispos*. **28**:246-254.

Hu M, Chen J, Zhu Y, Dantzig AH, Stratford RE and Kuhfeld MT Jr. (1994a) Mechanism and kinetics of transcellular transport of a new β-lactam antibiotic loracarbef across a human intestinal epithelial model system (Caco-2). *Pharm Res.* **11**:1405-1413.

Hu M, Chen J, Tran D, Zhu Y and Leonardo G (1994b) The Caco-2 Cell Monolayers as an intestinal metabolism model: metabolism of dipeptide Phe-Pro. *J Drug Target.* **2**:79-89.

Hu M, Chen J, and Lin H (2003) Disposition of Flavonoids via Recycling: Mechanistic Studies of Disposition of Apigenin in the Caco-2 Cell Culture Model. *J Pharmacol Exp Ther.* 307: 314-321.

Jeong EJ, Lin H, Hu M (2004) Disposition mechanisms of raloxifene in the human intestinal Caco-2 model. J Pharmacol Exp Ther. 310(1):376-85.

Jia X, Chen J, Lin H, Hu M (2004) Disposition of flavonoids via enteric recycling: enzyme-transporter coupling affects metabolism of biochanin A and formononetin and excretion of their phase II conjugates, *J Pharmacol Exp Ther*.**310**(3):1103-1113.

Jones C (1997) Clinical pharmacology & biopharmaceutical review for EVISTATM submitted to FDA (NDA 20-815).

Kemp DC, Fan PW and Stevens JC (2002) Characterization of raloxifene glucuronidation in vitro: contribution of intestinal metabolism to presystemic clearance. *Drug Metab Dispos.* **30**:694-700.

King CD, Rios GR, Green MD, Tephly TR (2000) UDP-glucuronosyltransferases. *Curr Drug Metab.* **1:**143-61.

Kubatka P, Bojkova B, Kalicka K, Chamilova M, Adamekova E, Ahlers I, Ahlersova E, Cermakova M (2001) Preventive effects of raloxifene and melatonin in N-methyl-N-nitrosourea-induced mammary carcinogenesis in female rats. *Neoplasma*. **48:**313-9.

Lacey JV Jr, Mink PJ, Lubin JH, Sherman ME, Troisi R, Hartge P, Schatzkin A, Schairer C (2002) Menopausal hormone replacement therapy and risk of ovarian cancer. JAMA. 288(3):334-341.

Lindstrom TD, Whitaker NG and Whitaker GW (1984) Disposition and metabolism of a new benzothiophene antiestrogen in rats, dogs and monkeys. *Xenobiotica*. **14**:841-847.

Liu Y, Hu M (2002) Absorption and metabolism of flavonoids in the caco-2 cell culture model and a perused rat intestinal model. *Drug Metab Dispos.* **30:**370-7.

Merchenthaler I, Funkhouser JM, Carver JM, Lundeen SG, Ghosh K, Winneker RC (1998) The effect of estrogens and antiestrogens in a rat model for hot flush. *Maturitas.* **30:**307-16.

Ozgonul M, Oge A, Sezer ED, Bayraktar F, Sozmen EY (2003) The effects of estrogen and raloxifene treatment on antioxidant enzymes in brain and liver of ovarectomized female rats. *Endocr Res* **29:**183-9.

Rossouw JE, Anderson GL, Prentice RL, LaCroix AZ, Kooperberg C, Stefanick ML, Jackson RD, Beresford SA, Howard BV, Johnson KC, Kotchen JM, Ockene J; Writing Group for the Women's Health Initiative Investigators (2002) Risks and benefits of estrogen plus

progestin in healthy postmenopausal women: principal results from the eomen's health initiative randonmized controlled trial. *JAMA.* **288**:321-333.

Setchell KD, Brown NM, Desai P, Zimmer-Nechemias L, Wolfe BE, Brashear WT, Kirschner AS, Cassidy A, Heubi JE (2001) Bioavailability of pure isoflavones in healthy humans and analysis of commercial soy isoflavone supplements. *J Nutr.* **131:**1362S-75S.

Setchell KD, Brown NM, Desai PB, Zimmer-Nechimias L, Wolfe B, Jakate AS, Creutzinger V, Heubi JE (2003) Bioavailability, disposition, and dose-response effects of soy isoflavones when consumed by healthy women at physiologically typical dietary intakes. *J Nutr.* **133:**1027-35.

Snyder KR, Sparano N, Malinowski JM (2000) Raloxifene hydrochloride. *Am J Health Syst Pharm.* **57:**1669-1675.

Strassburg CP, Kneip S, Topp J, Obermayer-Straub P, Barut A, Tukey RH, Manns MP(2000) Polymorphic gene regulation and interindividual variation of UDP-glucuronosyltransferase activity in human small intestine. *J Biol Chem.* **275**:36164-36171.

Strassburg CP, Manns MP, Tukey RH (1998) Expression of the UDP-glucuronosyltransferase 1A locus in human colon. Identification and characterization of the novel extrahepatic UGT1A8. *J Biol Chem.* **273**:8719-8726.

Strassburg CP, Nguyen N, Manns MP and Tukey RH (1999) UDP-glucuronosyltransferase activity in human liver and colon. *Gastroenterology* **116:**149-160.

Tukey RH and Strassburg CP (2000) Human UDP-glucuronosyltransferases metabolism, expression, and disease. *Annu Rev Pharmacol Toxicol* **40:** 581-616.

Walle UK, Galijatovic A, Walle T (1999) Transport of the flavonoid chrysin and its conjugated metabolites by the human intestinal cell line Caco-2. *Biochem Pharmacol.* **58:**431-438.

Zheng H, Kangas L, Harkonen PL (2004) Comparative study of the short-term effects of a novel selective estrogen receptor modulator, ospemifene, and raloxifene and tamoxifen on rat uterus. *J Steroid Biochem Mol Biol.* **88:**143-56.

FOOTNOTES:

This study was supported by National Institutes of Health (NIH) Grant CA 87779. The authors would like thank Dr. Vincent Tam and Mr. Yousif Rojeab for performing data fitting used in Figure 5.

[2]Present Address: Korea Institute of Toxicology, Daejeon, Republic of Korea

[3]Present Address: Departments of Behavioral Neuroscience, Oregon Health and Science University, Portland, Oregon

[4]Present Address: Department of Pharmacological and Pharmaceutical Sciences, College of Pharmacy, University of Houston, Houston, TX 77030

FIGURE LEGENDS:

Fig. 1. Representative HPLC profiles of raloxifene and its metabolites. Panel A, Panel B and Panel C show the peaks of major metabolites formed by female rat and human liver microsomes and UGT1A10, respectively. Two metabolites, M1 and M2, were identified as 6-β-glucuronide and 4'-β-glucuronide, since UGT1A10 was reported to produce only 4'-β-glucuronide (Kemp et al., 2002). The retention times for raloxifene, 6-β-glucuronide, 4'-β-glucuronide, and internal standard (testosterone) are 13.6, 7.2, 9.8 and 21.4 min, respectively.

Fig. 2. RT-PCR Analysis of UGT isoform specific RNAs in the Caco-2 cells. The bands (from left to right) correspond to house-keeping gene (b-actin) (lane 1), UGT1A (2), UGT1A1 (3), UGT1A3 (4), UGT1A4 (5), UGT1A5 (6), UGT1A6 (7), UGT1A7 (8), UGT1A8 (9), UGT1A9 (10), UGT1A10 (11), UGT1A3-5 (12), UGT1A 7-10 (13), positive control (14), DNA ladder (15).

Fig. 3. Rate of raloxifene glucuronidation (pmol/min/mg) by human (panel A) and rat (panel B) microsomes. Raloxifene (8.7 μM) was added to the microsomes with cofactors as described in *Materials and methods*. Incubation was carried out at 37ºC for 2 h. Solid and shaded columns represent the rate of glucuronidation for M1 and M2, respectively. FHLM, FHJM and FHIM represent pooled female human liver, jejunal and ileal microsomes, respectively (Panel A). FRLM, FRDM, FRJM, FRIM and FRCM represents pooled female rat liver, duodenal, jejunal, ileal and colonal microsomes, respectively (Panel B). Each column represents the mean of three determinations and the error bars are standard deviations of the mean. Star symbols indicate a statistically significant difference (or $p < 0.05$) between M1 and M2 formation.

Fig. 4. Effects of Concentration on raloxifene glucuronidation by human liver and intestinal microsomes for M1 (Panel A) and M2 (Panel B). Raloxifene (0.87~34.7 μM) was added to the microsomes with cofactors as described in *Materials and methods.* Incubation was carried out at 37ºC for 30 – 60 min depending on the concentration of raloxifene. FHLM, FHJM and FHIM represent pooled female human liver, jejunal and ileal microsomes, respectively. Each data point represents the mean of three determinations and the error bars are standard deviations of the mean. Each curve was obtained by nonlinear regression of the data points using SigmaPlot™.

Fig. 5. Effects of concentration on raloxifene glucuronidation by rat liver and intestinal microsomes for M1 (Panel A-E) and M2 (Panel F-J). Raloxifene (0.87~34.7 μM) was added to the microsomes with cofactors as described in *Materials and methods*. Incubation was carried out at 37ºC for 30 – 60 min depending on the concentration of raloxifene. FRLM, FRDM, FRJM, FRIM and FHCM represent pooled female rat liver, duodenal, jejunal, ileal and colonal microsomes, respectively. Each data point represents the mean of three determinations and the error bars are standard deviations of the mean. Each curve was obtained by nonlinear regression of the data points using ADAPT II.

Fig. 6. Eadie-Hofstee plot of concentration effect on raloxifene glucuronidation by rat liver and intestinal microsomes for M1 (Panel A-E) and M2 (Panel F-J). FRLM, FRDM, FRJM, FRIM and FHCM represent pooled female rat liver, duodenal, jejunal, ileal and colonic microsomes, respectively. Each data point represents the mean of three determinations and the error bars are standard deviations of the mean. Metabolite formation profiles by rat intestinal microsomes (except M2 formation by FRCM) showed substrate inhibition.

Fig 7. Inhibitory effect of genistein (Panel A) and apigenin (Panel B) on glucuronidation of raloxifene by human jejunal microsomes, rat jejunal microsomes, and Caco-2 cell lysate. Raloxifene (4.34 μM) and inhibitor (0~100 μM genistein or apigenin) were added to the microsomes or Caco-2 cell lysate with cofactors as described in "Materials and Methods." Incubation was carried out at 37ºC for 1 h (microsomes) or 4 h (Caco-2 cell lysate). Each data point represents the mean of three determinations and the error bars are standard deviations of the mean. The mean control values (± S.D.) of rate of glucuronidation (in pmol/min/mg protein) were 64.2 ± 0.7 (M1, human, genistein), 530.9 ± 15.7 (M2, human, genistein), 116. 3 ± 9.1 (M1, rat, genistein), 30.1 ± 2.3 (M2, rat, genistein), 0.626 ± 0.075 (M1, Caco-2, genistein), 0.446 ± 0.044 (M2, Caco-2, genistein), 46.6 ± 17.3 (M1, human, apigenin), 500.4 ± 28.3 (M2, human, apigenin), 343.2 ± 13.3 (M1, rat, apigenin), 87.8 ± 2.4 (M2, rat, apigenin), 0.599 ± 0.072 (M1, Caco-2, apigenin) and 0.427 ± 0.042 (M2, Caco-2, apigenin), respectively. Each curve was obtained by nonlinear regression of the data points using SigmaPlot™.

DMD Fast Forward. Published on March 15, 2005 as DOI: 10.1124/dmd.104.001883
This article has not been copyedited and formatted. The final version may differ from this version.

Table 1: PCR Primers for House-Keeping Gene and Human UGT1A Family. Some primers were designed based on work of Tukey and his coworkers (e.g., Strassburg et al, 1999).

Fragment	Acccession No. (GenBank)	Sequence (5' - 3')	Position (bases)	Expected Size
Beta-actin	M10278	GGCGGCACCACCATGTACCCT	942-962	
		CGATCCACACGGAGTACTTGC	1045-1065	124
UGT1	M57899	TCGAATCTTGCGAACAACACG	1042-1062	
		ATCATCACCATGGGAACGCC	1168-1187	146
1A1	M57899	AACAAGGAGCTCATGGCCTCC	412-432	
		CATGCAAGAAGAATACAGTGG	515-535	124
1A3	M84127	TGGTCTATCATAGGTCTTGTG	495-515	
		AACCACATCAAAGGAAGTAGC	557-577	83
1A4	M57951	GAAGGAATTTGATCGCGTTAC	287-307	
		GGCCTCATTATGCAGTAGCTC	417-437	151
1A5	M84129	CCCTGGAGGTGAATATGTA	299-317	
		AGAACGATTGAGTGTGACC	397-415	117
1A6	M84130	GGCCTACCATCTGTGTACCTC	703-723	
		TAGGACACAGGGTCTGGGCT	766-785	83
1A7	U39570	GGACGGCACCATTGCGAAG	458-476	
		CAAACTCCTGCAATTTAA	538-556	99
1A8	U42604	GGAATAGGTTGCCACTATCT	774-793	
		AGTCATGGCATCTGAGAACC	850-869	96
1A9	S55985	GGAACATTTATTATGCCACCG	679-699	
		TGGCTGTAGAGATCATACTCC	754-774	96
1A10	U39550	CCAATGATCTCTTAGGGTTCT	851--871	
		AATGGTCCTCCAAGTGCACGA	978-998	148
1A3-5	M57951	ACATGCTCTACCCTCTGGCCC	667-687	
		CACCACTGACACCTCTCTCTG	747-767	101
1A7-10	S55985	CAGTGCCCTGCTCCTCTTTCC	578-598	
		AAGTGCATGATGTGGTTCCGT	655-675	98

DMD Fast Forward. Published on March 15, 2005 as DOI: 10.1124/dmd.104.001883
This article has not been copyedited and formatted. The final version may differ from this version.

Table 2. Metabolic parameters of raloxifene glucuronidation by liver and intestinal microsomes in human and rat. Raloxifene was added to the microsomes with cofactors as described in Materials and methods. Apparent K_m, V_{max} and CL_{int} values were obtained by nonlinear regression of the data points in Fig. 4 and Fig. 5.

Species	Glucuronide	**Site**	**Apparent K_m (K_{si}) [c] (μM)**	**Apparent V_{max} (pmol/min/mg)**	**Apparent CL_{int} (μl/min/mg)**
Human	**M1**	liver[a]	14.48	1183	82
		jejunum[a]	4.89	348	71
		ileum[a]	8.72	424	49
	M2	liver[a]	3.63	747	206
		jejunum[a]	3.68	3711	1008
		ileum[a]	4.88	3871	793
Rat	**M1**	liver[a]	3.04	603	199
		duodnum[b]	2.42 (26.00) [c]	750	309
		jejunum[b]	1.40 (44.31) [c]	419	300
		ileum[b]	0.95 (47.80) [c]	117	124
		colon[b]	0.85 (74.27) [c]	145	170
	M2	liver[a]	4.39	161	37
		duodnum[b]	13.98 (4.76) [c]	678	49
		jejunum[b]	11.93 (6.09) [c]	368	31
		ileum[b]	3.518 (23.83) [c]	39	11
		colon[a]	0.77	23	30

[a.] The parameters were calculated from the data up to 34.7 μM raloxifene using the Michaelis-Menten equation.

[b.] The parameters were calculated according to equation (3) as described in Materials and Methods since it showed substrate inhibition (see results).

[c.] The constant describing the substrate inhibition interaction (K_{si}) calculated according to equation (3) as described in Materials and Methods.

Table 3. Inhibitory effect of genistein and apigenin on glucuronidation of raloxifene by human and rat jejunal microsomes and Caco-2 cell lysate. Raloxifene (4.34 μM) and inhibitor (0~100 μM genistein or apigenin) were added to the microsomes with cofactors as described in Materials and methods. Apparent 50% inhibitory concentration (IC_{50}) values were obtained by nonlinear regression of the data presented in Fig. 7 using SigmaPlot™.

Compound	Microsome	Glucuronide	Apparent IC_{50} (μM)
Genistein	Human jejunum	M1	51.57
		M2	44.90
	Rat jejunum	M1	4.66
		M2	9.42
	Caco-2 cell lysate	M1	7.78
		M2	8.19
Apigenin	Human jejunum	M1	14.80
		M2	16.70
	Rat jejunum	M1	5.02
		M2	3.39
	Caco-2 cell lysate	M1	1.87
		M2	2.14

DMD Fast Forward. Published on March 15, 2005 as DOI: 10.1124/dmd.104.001883
This article has not been copyedited and formatted. The final version may differ from this version.

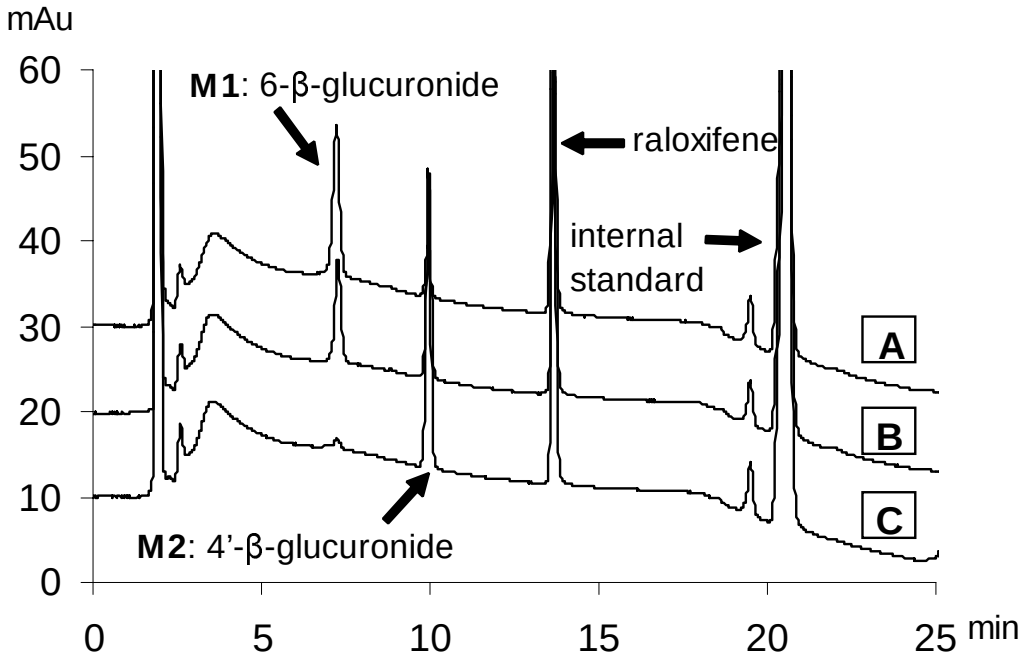

Fig. 1

DMD Fast Forward. Published on March 15, 2005 as DOI: 10.1124/dmd.104.001883
This article has not been copyedited and formatted. The final version may differ from this version.

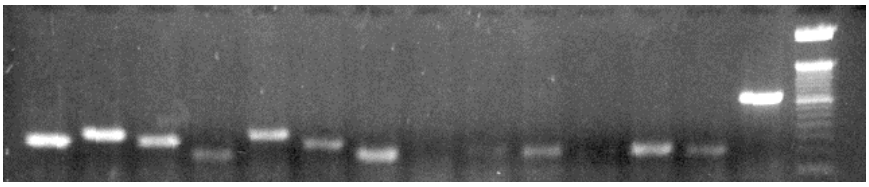

1 2 3 4 5 6 7 8 9 10 11 12 13 14 15 Lane No.

Fig. 2

DMD Fast Forward. Published on March 15, 2005 as DOI: 10.1124/dmd.104.001883
This article has not been copyedited and formatted. The final version may differ from this version.

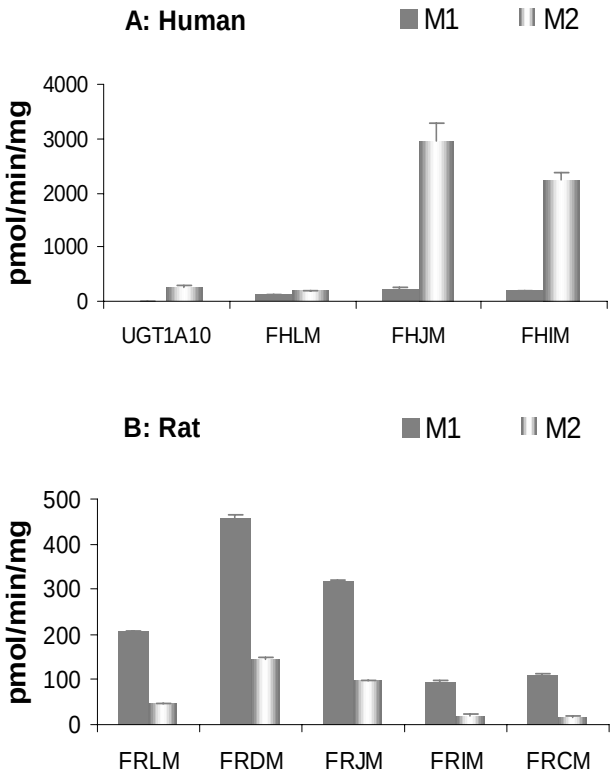

Fig. 3

DMD Fast Forward. Published on March 15, 2005 as DOI: 10.1124/dmd.104.001883
This article has not been copyedited and formatted. The final version may differ from this version.

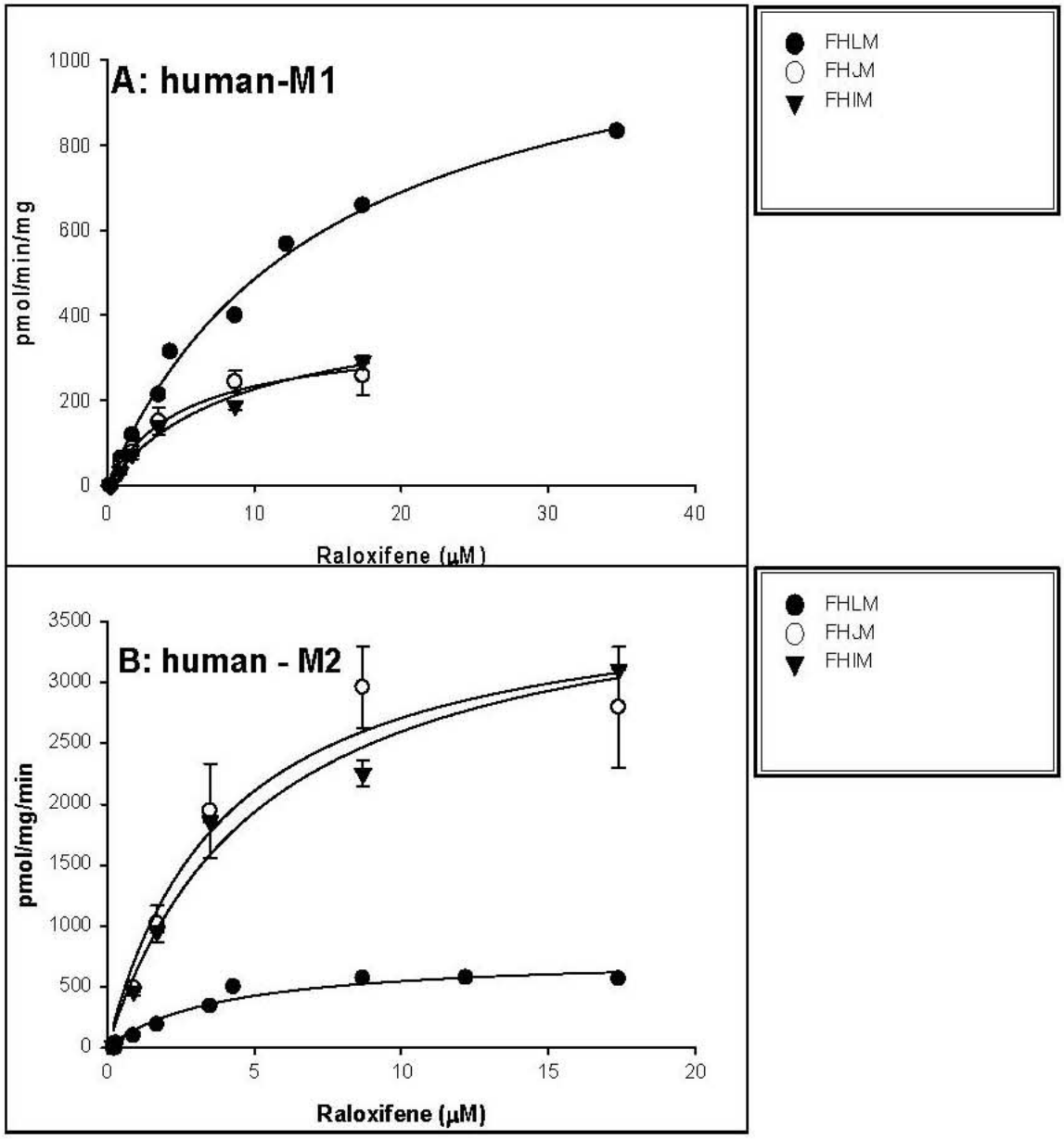

Fig. 4

DMD Fast Forward. Published on March 15, 2005 as DOI: 10.1124/dmd.104.001883
This article has not been copyedited and formatted. The final version may differ from this version.

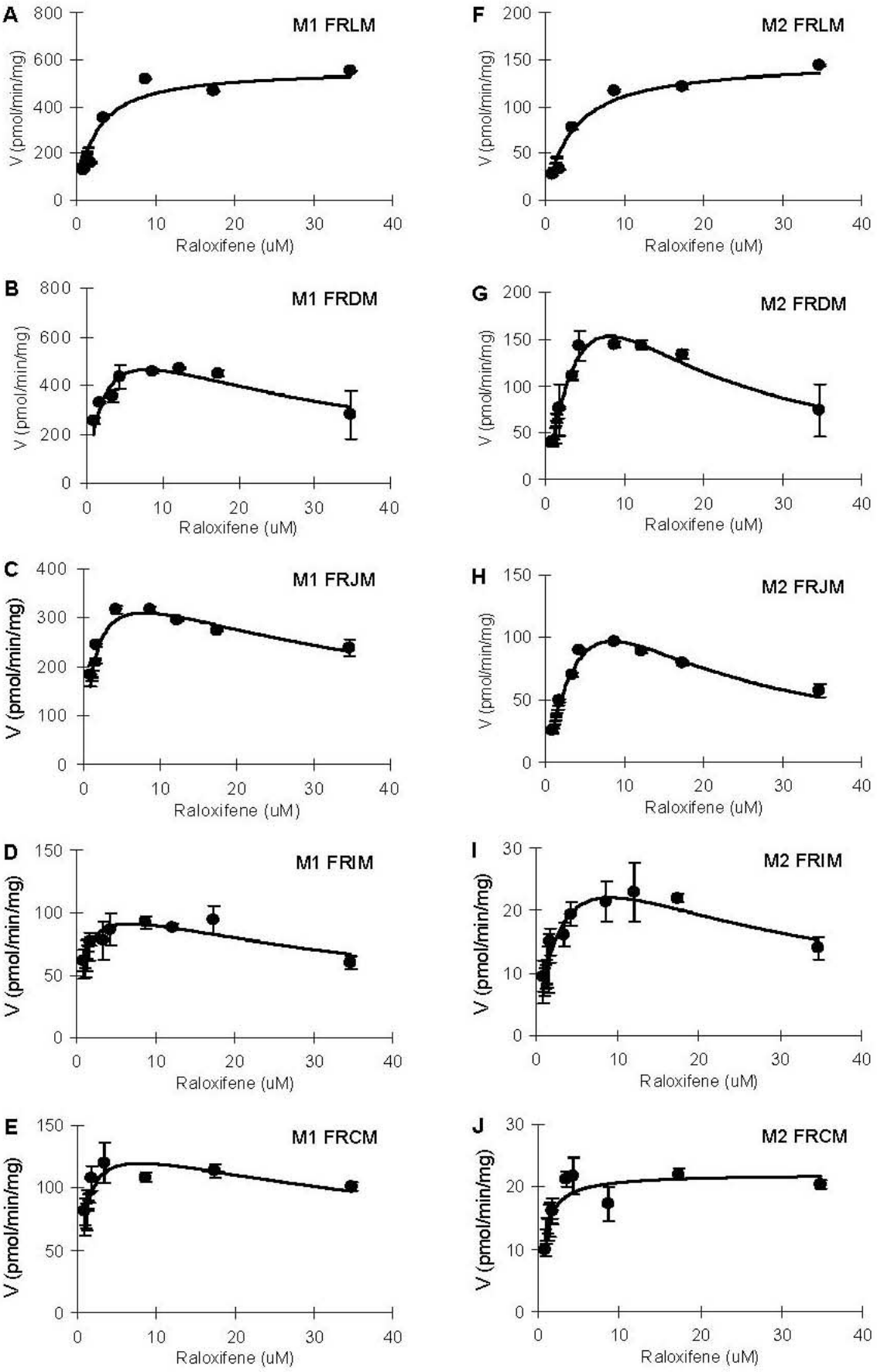

Fig. 5

DMD Fast Forward. Published on March 15, 2005 as DOI: 10.1124/dmd.104.001883
This article has not been copyedited and formatted. The final version may differ from this version.

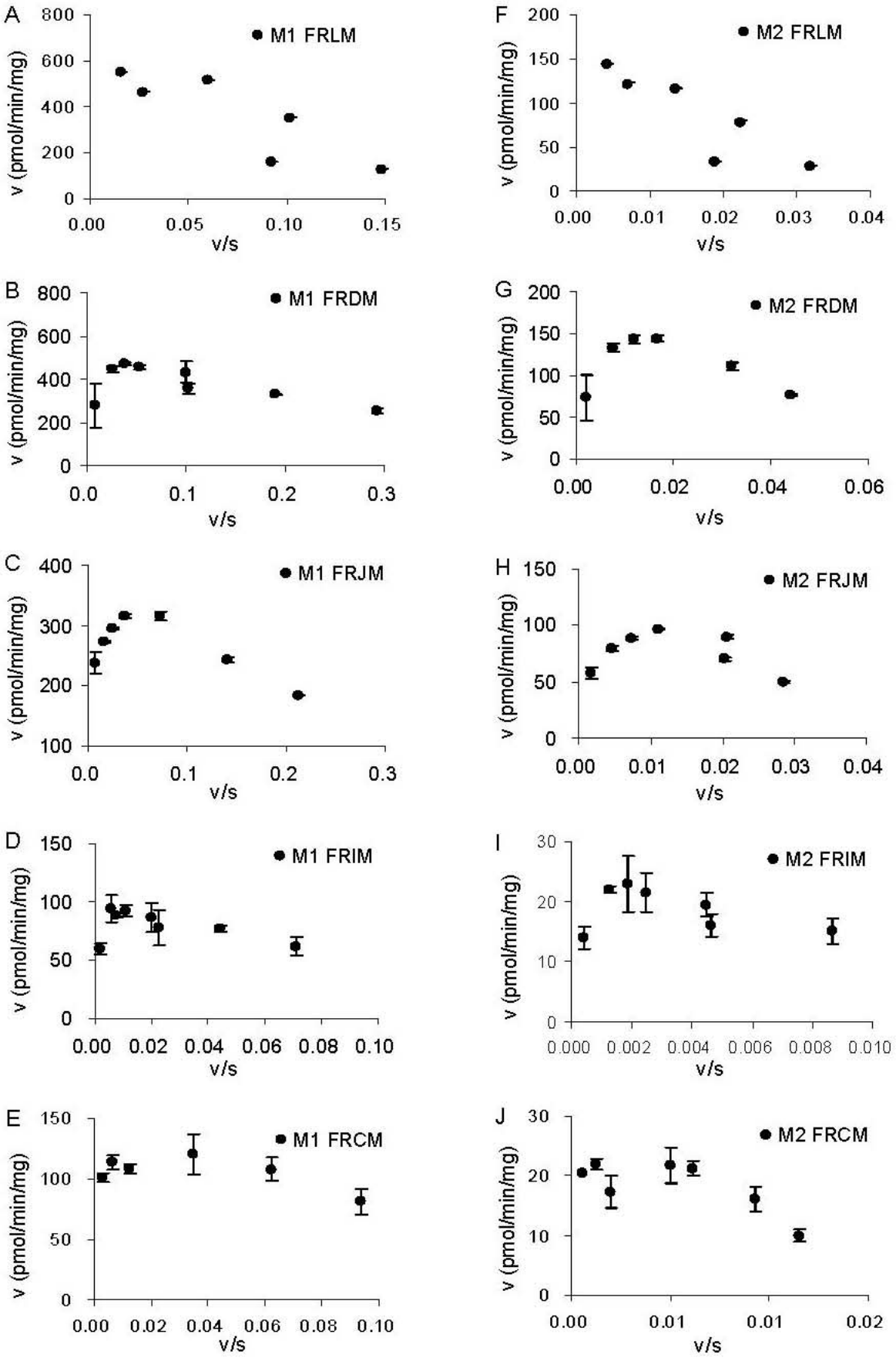

Fig. 6

DMD Fast Forward. Published on March 15, 2005 as DOI: 10.1124/dmd.104.001883
This article has not been copyedited and formatted. The final version may differ from this version.

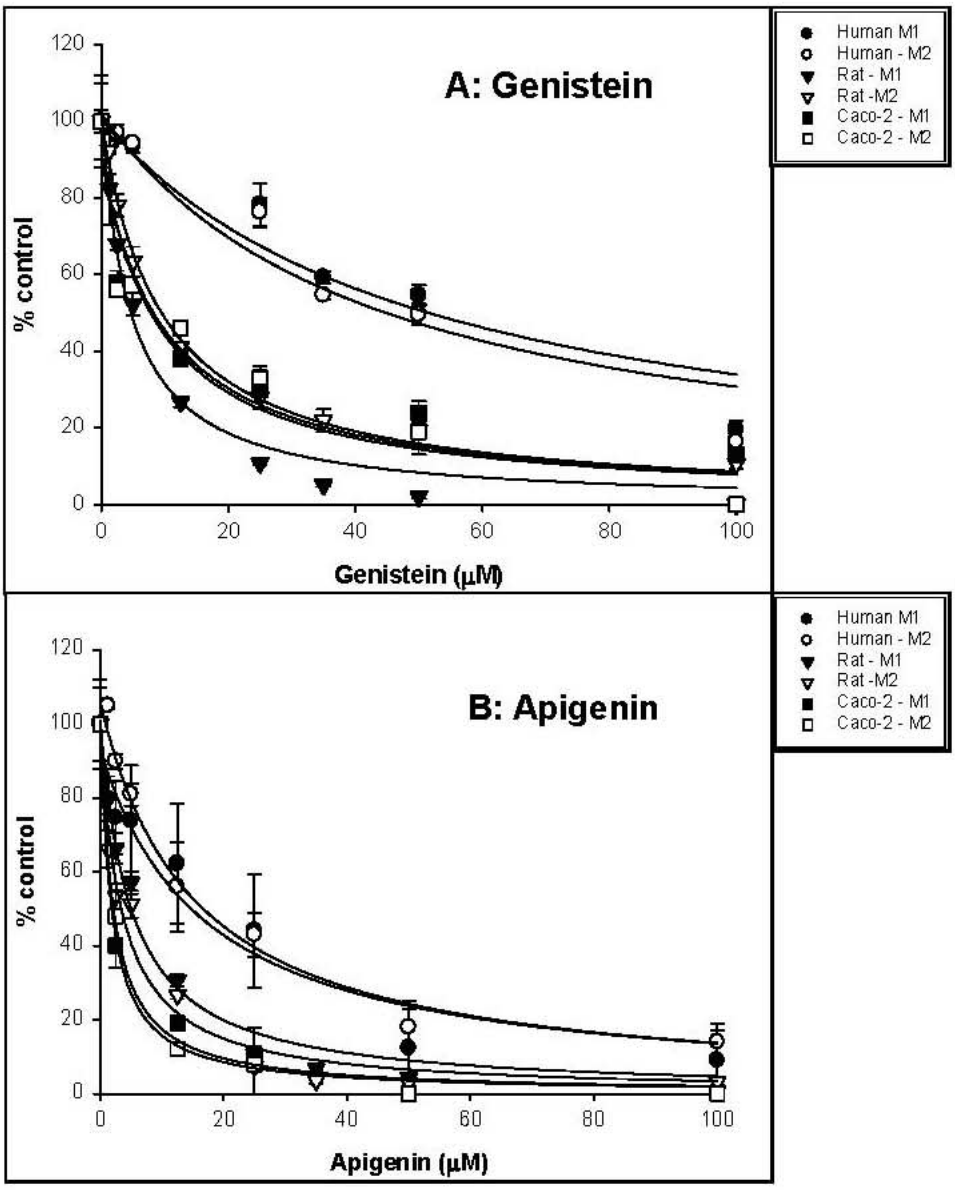

Fig. 7